

Cross-Relaxation in Electron–Nuclear Coupled Systems by Pulsed Dynamic Nuclear Polarization at Low Magnetic Fields

B. M. Odintsov,^{*,†,§} R. L. Belford,^{†,‡} and R. B. Clarkson^{†,§}

Illinois EPR Research Center, Department of Chemistry, and Department of Veterinary Clinical Medicine, University of Illinois, 190 MSB, 506 S. Mathews, Urbana, Illinois 61801

Received: August 23, 1996; In Final Form: October 22, 1996[⊗]

A new method for the experimental determination of the cross-relaxation (CR) transition rates in liquid solutions of paramagnetic compounds has been developed utilizing a pulsed dynamic nuclear polarization (DNP) technique. In contrast to NMR relaxation, which is proportional to the sum of relaxation rates, the DNP effect is determined by the ratio of transition rates in the nucleus–electron coupled spin system. By use of pulsed DNP, the NMR relaxation rates and DNP data can be obtained in the same experiment. As a result, a set of independent equations for CR and dipole–dipole (DD) transition rates can be derived. The solution of these equations defines individual cross-relaxation and DD transition rates, as well as molecular–kinetic information, and avoids the necessity of performing complicated variable frequency and temperature measurements. A pulsed DNP relaxometer operating at a proton frequency of 0.5 MHz was constructed. The 4-oxo-2,2,6,6-tetramethyl-1-piperidinyloxy (TEMPONE) stable free radical in benzene was chosen for study as a system with strong intermolecular dipole–dipole interactions. The measurement of individual rates of CR and DD transitions gave us the distance ($b = 5.0 \text{ \AA}$) between spins I and S for the solvated radical of TEMPONE and also the molecular rotational correlation time ($\tau_r = 2.5 \times 10^{-10} \text{ s}$). Another system studied was the solvated electron in hexamethylphosphorus amide (HMPA) in which scalar and DD interactions are present at the same time. The basic characteristics of this fundamentally important elementary paramagnetic center have been obtained, such as the lifetime of HMPA molecules in the solvent cage ($\tau_h = 2.9 \times 10^{-9} \text{ s}$) and the intermolecular hyperfine constant value ($a = 0.08 \text{ MHz}$). Pulsed DNP is shown to be a valuable approach for the study of very weak hyperfine interactions that are not readily detected by other traditional magnetic resonance methods.

1. Introduction

It is well-known that the magnetic relaxation of nuclear spins in paramagnetic solutions can be caused by their interaction with electron spins. Cross-relaxation (CR) transitions involving simultaneous flips of electron and nuclear spins play the main role in these interactions.

Since the publication of the first work on CR by Bloembergen et al.,¹ a great deal of attention has been devoted to the problem of energy transfer between sublevels in magnetic spin systems consisting of species with different gyromagnetic ratios. On one hand, cross-relaxation is of great interest as a particular manifestation of the central problem of nonequilibrium statistical physics—the establishment of equilibrium in systems of many interacting bodies. On the other hand, CR processes form the foundation of different kinds of dynamic nuclear polarization (DNP) phenomena that are sensitive methods for studying the hyperfine interactions in paramagnetic solutions.

During the past few years there has been a renewal of interest in the problem of cross-relaxation in liquids in part because of the partial revision of traditional radical-pair and singlet–triplet mechanisms for chemically induced dynamic nuclear polarization, chemically induced dynamic electronic polarization (CIDEP), and stimulated nuclear polarization phenomena.^{2,3} The initial observation leading to a revision of these mechanisms was the unusual behavior of spin polarization in the CIDEP experiment,² which cannot be described in the framework of

the traditional mechanisms. The anomalies observed were explained in terms of CR processes in short-lived radicals.

The basic laws of CR have been explained by the perturbation theory approach.⁴ The problem of experimentally measuring the rates of different CR processes has not been solved satisfactorily. It is generally accepted that the rate constant for the buildup of DNP by the Overhauser mechanism⁴ is the nuclear spin–lattice relaxation time T_{1n} . Actually, the net effect of nucleus–electron interactions on DNP, as well as on T_{1n} , is the result of competition between different cross-relaxation and dipole–dipole transitions. In contrast to dipole–dipole relaxation, CR processes are very sensitive to the external magnetic field strength. Low magnetic fields are of special interest because it is in such an environment that the CR spectral density functions have the highest values.

The objective of the present work is to describe a new method of experimentally measuring the different CR probabilities by DNP in liquid solutions of paramagnetic compounds, utilizing a pulsed DNP approach at low magnetic fields.

2. Cross-Relaxation Rates

Since rapid molecular motion in a paramagnetic solution may permit all nuclei to interact with unpaired electrons, it is reasonable to describe the DNP phenomenon in the approximation of the two-spin nuclear–electronic model.^{4,5} Figure 1 shows the states in such a two-spin system and indicates the probabilities of the transitions between them. Relaxation transition P corresponds to the electronic Zeeman effect (EPR signal), q to the NMR signal, and s , r , and c to cross-relaxation involving simultaneous flips of electron and nuclear spins. It can be noted that the nuclear transition probability q consists of two

[†] Illinois EPR Research Center.

[‡] Department of Chemistry.

[§] Department of Veterinary Clinical Medicine.

[⊗] Abstract published in *Advance ACS Abstracts*, December 1, 1996.

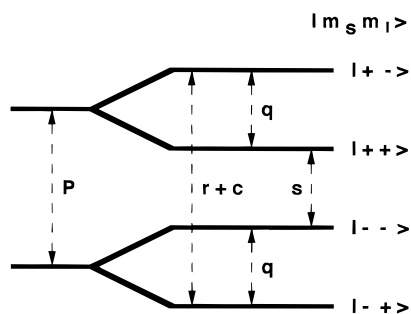


Figure 1. Scheme of energy states and probabilities of transitions in terms of two-spin (I–S) model. It is assumed that the nuclear Zeeman energy is greater than the intermolecular electronic–nuclear hyperfine interaction and that the magnetogyric ratio of the nucleus is positive.

components: $q = q'' + q'$, where q'' is the result of the nucleus–electron interaction and q' of nuclear–nuclear interactions.

In the coupled nuclear–electronic system the time dependence of NMR polarization enhancement $\langle I_z \rangle$ can be described by the equation⁴

$$d\langle I_z \rangle / dt = -[(\langle I_z \rangle - I_0) - \xi f (\langle S_z \rangle - S_0)] / T_{1n} \quad (1)$$

where we use designations introduced by Abragam.⁴

The main DNP nuclear–electronic coupling parameter

$$\xi = (s - r - c) / (s + r + c + 2q'') \quad (2)$$

is the ratio of the difference in cross-relaxation transition probabilities to all the relaxation probabilities in the coupled system.

The nuclear spin–lattice relaxation time in a paramagnetic solution is represented by

$$T_{1n}^{-1} = s + r + c + 2q \quad (3)$$

and the leakage factor for nuclear spins is given by

$$f = 1 - T_{1n} / T_{1n}(0) \quad (4)$$

where $T_{1n}(0)$ is the nuclear spin–lattice relaxation time of pure solvent.

I_0 and S_0 in (1) represent the equilibrium nuclear and electronic magnetization, respectively.

The Hamiltonian for the nuclear–electronic interaction can be presented in the form

$$H_{IS}(t) = F(t)U \quad (5)$$

where operator U contains only spin components. In this case, the probability of relaxation transitions between $|m_s, m_I\rangle$ and $|m_s', m_I'\rangle$ sublevels in Figure 1 is given by the expression⁵

$$W = \hbar^{-2} |\langle m_s, m_I | U | m_s', m_I' \rangle|^2 J(\omega_{mm'}) \quad (6)$$

where $J(\omega_{mm'})$ is the spectral density of the time-dependent function $F(t)$ in (5) that determines the frequency ($\omega_{mm'}$) dependence of W for different models of spin motion.⁶ Matrix elements of the spin operator U in (6) determine what kinds of transitions are allowed for different types of spin–spin interactions.

There are two types of magnetic interactions that cause the relaxation transitions in the coupled nucleus–electron system. One of them is the dipole–dipole (DD) interaction between nuclear and electronic spins:

$$H_d = \gamma_S \gamma_I \hbar^2 [3(\mathbf{I} \cdot \mathbf{b})(\mathbf{S} \cdot \mathbf{b}) / b^5 - (\mathbf{I} \cdot \mathbf{S}) / b^3] \quad (7)$$

where b is the distance between I and S spins.

Another interaction is the scalar (contact) coupling, which is proportional to the unpaired electron density at the nucleus $|\Psi(0)|^2$:

$$H_S = a(\mathbf{I} \cdot \mathbf{S}) \quad (8)$$

where $a = (8\pi/3)\gamma_S \gamma_I \hbar^2 |\Psi(0)|^2$ is the contact hyperfine coupling constant. Using raising and lowering operators determined in ref 6, one can easily show from (6) that the DD interaction can initiate s , r , P , and q transitions in Figure 1, whereas the scalar interaction can lead only to the $c|+-\rangle \leftrightarrow |-+\rangle$ transition.

Using the results of the work of Hausser and Stehlik,⁵ one can find from (6) the expressions for DD transition probabilities in the approximation of the two-spin model:

$$s = \frac{3}{5\beta} J_d(\omega_S + \omega_I) \quad (9)$$

$$r = \frac{1}{10\beta} J_d(\omega_S - \omega_I)$$

$$q'' = \frac{3}{20\beta} J_d(\omega_I)$$

where $\beta = \gamma_S \gamma_I \hbar^2 / b^6$, $J_d(\omega) = \tau_r / (1 + \omega^2 \tau_r^2)$, τ_r is the correlation time characterizing the isotropic rotation of the paramagnetic species, ω_I and ω_S are the Larmor frequencies of the nuclear and electronic spin, respectively, and the other symbols have their usual meaning.

In the condition of “extreme narrowing”, $\omega_S \tau_r \ll 1$, the relation between DD relaxation probabilities can be obtained from (9):

$$s:r:q'' = 12:2:3 \quad (10)$$

As a result, the coupling parameter ξ in (2) is equal to its extreme DD value of +0.5.

If the “extreme narrowing” condition is not fulfilled, then the s and r transition probabilities, which both contain the electronic frequency ω_S , decrease with increasing ω_S , in contrast to q'' which does not contain ω_S and, consequently, stays constant as long as the much less severe condition $\omega_I \tau_r \ll 1$ is fulfilled. Finally, if $\omega_I \tau_r \ll 1$ no longer holds, q'' also decreases as ω_I increases. But in the case of low-viscosity liquids at room temperature, it approaches zero only at magnetic fields of 10^5 – 10^7 G. The value of parameter ξ for DD interactions decreases from +0.5 to 0 as $\omega_S \tau_r$ increases.

In the more complicated case of both DD and contact interactions being present simultaneously, an additional term c should be taken into account in (2) and (3). According to ref 4, this term can be described by the formula

$$c(\omega) = \frac{a^2}{2} J_S(\omega_S - \omega_I) \quad (11)$$

where, in the framework of a “sticking” model,⁵ $J_S(\omega) = \tau_h / (1 + \omega^2 \tau_h^2)$ and τ_h is the lifetime of spin I in the solvent cage

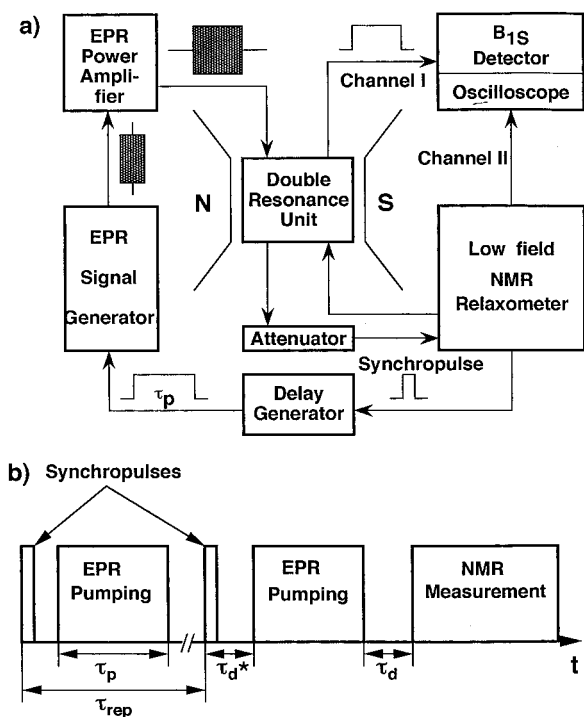


Figure 2. (a) Block diagram of the pulsed DNP instrument used at low magnetic field; (b) time sequences of EPR and NMR pulses in pulsed DNP experiment.

surrounding the spin *S*. The parameter ξ for the contact interaction changes from -1.0 to 0 as $\omega_S \tau_r$ increases.

3. Experimental Section

a. Equipment. The experimental setup for low-field DNP relaxation measurements is shown in Figure 2a. A portable NMR relaxometer⁷ was modified and used to detect the polarized NMR signal.

The double resonance unit consists of coaxial EPR and NMR coils. A spiral delay line (helix) was used to enhance the EPR saturating field. To provide the maximum level of B_{1S} inside the sample, the helix parameters were calculated according to ref 8 (special case of helix in screen). The large difference between EPR and NMR frequencies made it possible to use the NMR coil as a screen.

A two-channel Hewlett-Packard 54600A digital oscilloscope was used to provide display and averaging of the NMR signal amplitude (channel 1) and for measurement of the voltage on a high-frequency (HF) diode (channel 2) proportional to the B_{1S} value inside the EPR helix. The coefficient of proportionality between the voltage and B_{1S} has been determined in special experiments by using a 1 mM aqueous solution of Fremy's salt $K_2[NO(SO_3)_2]$ with known electronic relaxation times.⁹

Since the amplitude of the NMR signal in a DNP experiment can range over several orders of magnitude, a calibrated attenuator was used to prevent overloading of the NMR receiver.

A synchronizing pulse from the NMR relaxometer (Figure 2b) activates the delay generator, which provides the delay time τ_d between the EPR pumping pulse and NMR pulse sequences. At the same time, the delay generator creates the rectangular pulse that modulates the amplitude of a Hewlett-Packard 8647A signal generator, which is the source of the EPR resonance frequency. This rf pulse is then amplified by a Henry Radio 500 W power amplifier with a gain of 20. The period of the EPR saturating pulses can be chosen to avoid microwave heating of the sample.

b. Method. For many systems, it can be assumed that, on the scale of nuclear relaxation times, the electronic relaxation happens instantly. This assumption gives us the necessary initial conditions for the integration of eq 1. For a two-pulse Hahn NMR sequence generated after an EPR pumping pulse, the principal equation describing the relative amplitude enhancement A of the nuclear spin echo signal V derived from a polarized sample can be obtained from (1):

$$A = [V \exp(2\tau_1/T_2) - V_0]/V_0 = A_b Z [1 - \exp(-\tau_p/T_{1n})] \exp(-\tau_d/T_{1n}) \quad (12)$$

where V_0 is the amplitude of the nonpolarized echo, τ_p is the duration of the EPR saturating pulse, τ_1 is the time delay between 90° and 180° NMR pulses, $\tau_d = t - \tau_p$, $A_b = \xi f \gamma_S / \gamma_I$, and $Z = (S_0 - \langle S_z \rangle) / S_0$ is the saturation parameter, which depends on the EPR line shape. For the simplest case of a single Lorentzian EPR line saturated in the center,

$$Z = \gamma_S^2 B_{1S}^2 T_{1S} T_{2S} / (1 + \gamma_S^2 B_{1S}^2 T_{1S} T_{2S}) \quad (13)$$

In this case, one can derive from (12) and (13) that the reciprocal value of the NMR enhancement $A^{-1} [1 - \exp(-\tau_p/T_{1n})] \exp(-\tau_d/T_{1n})$ depends linearly on the inverse square of the EPR saturating field amplitude B_{1S}^{-2} . Parameters A_b and ξ were found experimentally by extrapolating this line to zero B_{1S}^{-2} value according to (12) and (13). The leakage factor f was obtained by measuring T_{1n} and $T_{1n}(0)$ in (4).

According to (12), the spin-lattice relaxation time T_{1n} can be measured in two ways—by changing either the polarization time τ_p or the delay time τ_d between the EPR pulse and the NMR pulse sequence. Both methods were utilized in these experiments. The spin-spin relaxation time T_2 was measured by the Carr-Purcell ($90^\circ - \tau_1 - 180^\circ - 2\tau_1 - 180^\circ \dots$) method. $T_{1n}(0)$ was obtained by a standard ($180^\circ - \tau - 90^\circ$) NMR method.^{7,10} By measurement of the dependence of the NMR polarized spin echo amplitude on the EPR pumping field frequency, it is possible to get the EPR "absorption" line shape at low magnetic fields by DNP.

Experiments were carried out under the following conditions: $\nu_1 = \omega_I / (2\pi) = 0.5$ MHz and $B_0 = 117$ G. The electron resonance frequency can be varied from 300 to 350 MHz. The major source of error in the DNP experiment arises from the inaccuracy of measuring the nonpolarized NMR signal intensity. By means of the averaging options of the HP 54600A oscilloscope, the relative experimental error was decreased to $\pm 5\%$.

Technically, the pulsed DNP method completely solves the problem, found in CW DNP experiments, of NMR detection path coupling to the strong EPR saturating field because it separates these two processes in time. Besides, the pulsed DNP regime permits a measurement of the leakage factor f (4) in the same magnetic field B_0 in which the DNP experiment is carried out. Thus, errors arising from the dependence of the leakage factor on the field B_0 are eliminated.

It should be noted that the DNP enhancement in liquids increases with decreasing external magnetic field strength because of the frequency dispersion of the spectral density functions in (6) that determine the probability of cross-relaxation transitions. Thus, the pulsed DNP method is especially effective in low magnetic fields, which is the area of special interest of this work.

c. Samples. The 4-oxo-2,2,6,6-tetramethyl-1-piperidinyloxy (TEMPO) stable free radical (purchased from Aldrich, Milwaukee, WI) in benzene was chosen for study as a system with strong dipole-dipole intermolecular interactions. Prior to measurement, the sample was bubbled with pure helium for 15

min. The radical concentration in solution was 5×10^{-2} M. An EPR spectrum of TEMPONE in low magnetic fields consisted of a simple triplet structure with the usual free radical g factor, close to the free electron value of 2.0023, and hyperfine splitting of about 15 G due to interaction with the ^{14}N nucleus.

Another system that was studied was the solvated electron in hexamethylphosphorus amide (HMPA) in which there are both scalar and DD interactions. A 10^{-2} M solution of metallic Na in HMPA was used as a source of solvated electrons. The EPR spectrum of solvated electrons in HMPA at room temperature consisted of an intense Lorentzian singlet with a line width of about 0.15 G and a g factor of 2.0021.

4. Results and Discussion.

It follows from eqs 2, 4, and 12 that the DNP phenomenon is strongly dependent on the ratios of transition probabilities in the coupled spin system but not directly on the probabilities themselves, in contrast to NMR relaxation. As a result, the use of both DNP and NMR relaxation data in pulsed DNP experiments gives us a set of independent equations for transition probabilities, providing much more information.

When analyzing the set of equations in (9), one finds that if the “extreme narrowing” condition $\omega_S \tau_r \ll 1$ is not fulfilled, then the $s(\omega_S + \omega_I)$ and $r(\omega_S - \omega_I)$ transition probabilities decrease with increasing ω_S , in contrast to $q''(\omega_I)$, which stays constant as long as the much less severe condition $\omega_I \tau_r \ll 1$ is fulfilled. At the same time, the relation $s/r = 6$ for protons is independent of frequency (within an error of $\pm 0.3\%$) because of the big difference between ω_S and ω_I (see eq 9). As a result, it is possible to write a system of equations

$$\begin{aligned} \xi &= (s - r - c)/(s + r + c + 2q'') \\ T_{1n}^{-1} &= s + r + c + 2q'' + 2q' \quad (14) \\ s/r &= 6 \end{aligned}$$

where $2q' = T_{1n}(0)^{-1}$.

Oscillograms of the DNP effect in a 50 mM solution of TEMPONE stable free radical in benzene are shown in Figure 3. Pulsed EPR pumping at a resonance frequency of 330 MHz leads to a large change in the benzene proton NMR spin echo signal and leads to a high negative signal enhancement as a result of strong dipole–dipole hyperfine interactions. Extrapolation of the saturation curve in Figure 4 to $B_{1S}^{-2} \rightarrow 0$ in accordance with (12) and (13) gives us A_b and the nucleus–electron coupling parameter $\xi = +0.46$, which is close to the extreme DD value of +0.5. NMR relaxation times were measured by methods described above and are shown in Table 1.

One can find from (14) that in the case of DD interactions ($c = 0$)

$$\begin{aligned} s &= 1.2\xi[T_{1n}^{-1} - T_{1n}(0)^{-1}] \\ r &= 0.2\xi[T_{1n}^{-1} - T_{1n}(0)^{-1}] \quad (15) \\ q'' &= 0.1[T_{1n}^{-1} - T_{1n}(0)^{-1}](5 - 7\xi) \end{aligned}$$

The equations in (15) provide a route to calculate from experimental DNP relaxation data the individual cross-relaxation and DD probabilities at any magnetic field strength.

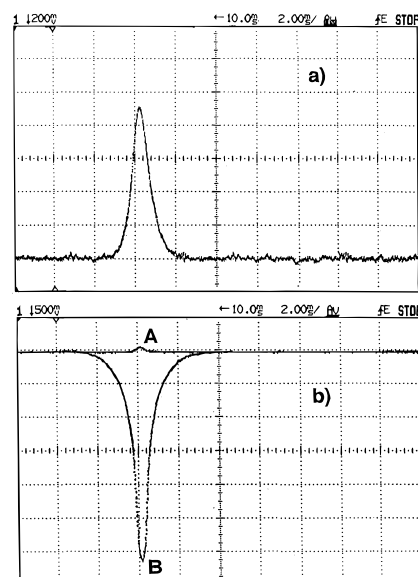


Figure 3. (a) Proton NMR echo signal in 0.05 M TEMPONE–benzene solution at $B_0=117$ G without EPR pumping ($B_{1S} = 0$, $\tau_1 = 8$ ms); (b) curve A is for the same NMR echo signal with a 20-fold decrease of NMR receiving channel sensitivity, and curve B is for negative proton echo signal polarization in TEMPONE–benzene solution as a result of DD intermolecular interactions ($B_{1S} = 1.2$ G, $\tau_1 = 8$ ms, $\tau_p = 100$ ms, $\tau_d = 0$).

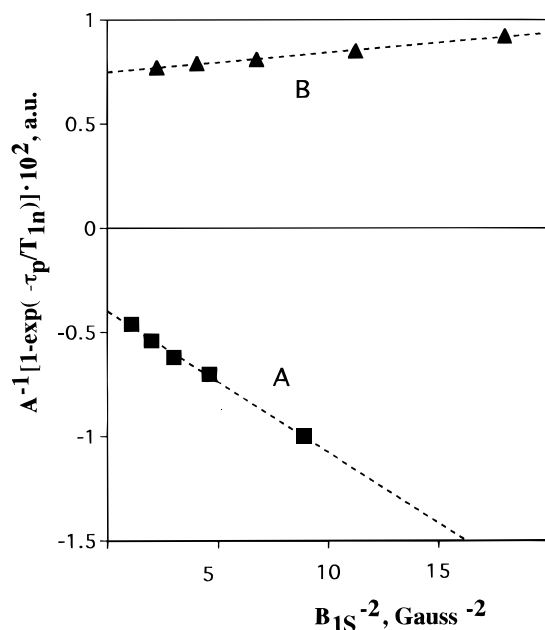


Figure 4. Plots of experimental EPR saturation: (A) 0.05 M solution of TEMPONE radical in benzene; (B) 0.01 M solution of solvated electrons in HMPA.

Using (15), one finds the CR and DD transition probabilities for TEMPONE radical in benzene:

$$s = 1.55 \text{ s}^{-1}, \quad r = 0.26 \text{ s}^{-1}, \quad q'' = 0.50 \text{ s}^{-1} \quad (16)$$

Relation 10 is thus transformed to

$$s:r:q'' = 9.3:1.6:3 \quad (17)$$

The cross relaxation rates s and r at $B_0 = 117$ G are smaller than those at zero magnetic field.

Now it is possible from (16) and (9) to calculate the rotational correlation time τ_r of the solvated complex and estimate the distance between spins I and S in a solvated TEMPONE radical

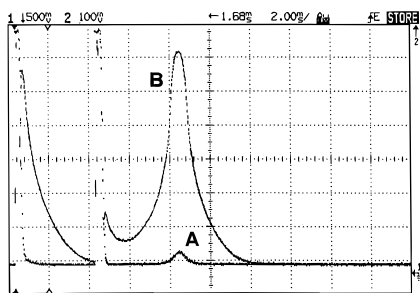


Figure 5. Positive proton echo signal polarization in 0.01 M solution of solvated electrons in HMPA as a result of scalar intermolecular interactions: (A) $B_{1S} = 0$; (B) $B_{1S} = 0.2$ G, $\tau_1 = 4$ ms, $\tau_p = 100$ ms, $\tau_d = 0$.

TABLE 1: Experimental DNP Relaxation Data at Magnetic Field $B_0 = 117$ G and Molecular–Kinetic Parameters of the Investigated Compounds

parameters	TEMPONE in benzene	solvated electron in HMPA
A_b	-290 ± 14.5	$+131 \pm 6.6$
ξ	$+0.46 \pm 0.02$	-0.60 ± 0.03
f	0.97 ± 0.05	0.33 ± 0.02
T_{1n}, s	0.35 ± 0.02	1.00 ± 0.05
T_{2n}, s	0.32 ± 0.02	0.18 ± 0.01
s, s^{-1}	1.55 ± 0.08	$0.050 \pm 3 \times 10^{-3}$
r, s^{-1}	0.26 ± 0.02	$0.008 \pm 4 \times 10^{-4}$
q'', s^{-1}	0.50 ± 0.03	0.016 ± 10^{-3}
c, s^{-1}		0.24 ± 10^{-2}
τ_r, s	$2.5 \times 10^{-10} \pm 1.5 \times 10^{-11}$	$2.2 \times 10^{-10} \pm 10^{-11}$
τ_h, s		$2.9 \times 10^{-9} \pm 2 \times 10^{-10}$
a, MHz		$0.08 \pm 4 \times 10^{-3}$

in the approximation of the two-spin model. Calculations give $\tau_r = 2.5 \times 10^{-10}$ s and $b \approx 5.0$ Å.

A more complex situation arises in the system in which scalar and DD interactions are present simultaneously. The solvated electron in HMPA is an example of this more complex case.

The DNP of alkali metals in liquid ammonia has been studied extensively. It was revealed that alkali metal atoms often give up the valence electron easily, which then interacts with the solvent as an individual particle.¹¹ At the same time, there is a lack of data on DNP of solvated electrons in organic solutions because of the extreme temperature instability of such systems and their strong microwave heating under CW EPR saturation. It is clear that the investigation of hyperfine interactions and molecular dynamics of the unique elementary e^- paramagnetic center in organic solvents is of particular interest. Pulsed DNP gives us a possibility of avoiding rf heating and the consequent destruction of such systems during spectroscopic observation.

Pulsed EPR pumping of solvated electrons at the Larmor electron frequency leads to positive proton polarization (Figure 5) as a result of strong scalar intermolecular coupling. Experimental DNP data are shown in Table 1. In contrast to the TEMPONE radical in benzene, the solvated electron system shows a large difference between spin–spin (T_{2n}) and spin–lattice (T_{1n}) proton relaxation times, which is typical for systems with scalar interactions. In accordance with eqs 3 and 11 and by use of the results of ref 4, it is possible to represent the relaxation times for this system in the form

$$T_{1n}^{-1} = DD + c$$

$$T_{2n}^{-1} = DD + c/2 + c(0)/2 \quad (18)$$

where $DD = s + r + 2q$ is the sum of dipole–dipole transitions probabilities and $c(0) = a^2 J_S(0)$.

From (10), taking into account the frequency dependence of DD transitions, one can derive the following:

$$s:r:q'' = 12(1 + \omega_S^2 \tau_r^2)^{-1} : 2(1 + \omega_S^2 \tau_r^2)^{-1} : 3 \quad (19)$$

simplifying the expressions, since $\omega_S \gg \omega_r$. Using (19), one can obtain from (14) the dependence of the scalar term c on the value of the rotational correlation time τ_r :

$$c = (T_{1n}^{-1} - T_{1n}(0)^{-1}) [5 - \xi(10 + 3\omega_S^2 \tau_r^2)] / 3(5 + \omega_S^2 \tau_r^2) \quad (20)$$

Using experimental data in Table 1, one can show that at the EPR resonance frequency of 330 MHz, changes in the correlation time τ_r over the region from 10^{-8} to 10^{-12} s result in relatively small changes in the value of c (about 8%). Such weak scalar relaxation dependence on τ_r is quite understandable because isotropic scalar coupling cannot be modulated by rotation and depends only on the lifetime τ_h of the solvent molecule in the solvent cage of the paramagnetic particles. As the scalar interaction decreases and the coupling parameter ξ increases from -1 to 0 , respectively, the dependence between ξ and τ_r becomes stronger.

Expression 20 gives us $c = 0.24$ s⁻¹ as the scalar transition probability value for solvated electrons in HMPA. It is easy now to calculate from (14) the DD transition probabilities

$$r = 0.2 \{ \xi [T_{1n}^{-1} - T_{1n}(0)^{-1}] + c \}$$

$$q'' = 0.1 \{ [T_{1n}^{-1} - T_{1n}(0)^{-1}] (5 - 7\xi) - 12c \}$$

$$s = 1.2 \{ \xi [T_{1n}^{-1} - T_{1n}(0)^{-1}] + c \} \quad (21)$$

and estimate the rotational correlation time $\tau_r = 2.2 \times 10^{-10}$ s of the solvated electron. By use of the value of c obtained above, the difference between the experimental proton T_{1n} and T_{2n} relaxation times (see Table 1), and (18) and (11), one can find the lifetime $\tau_h = 2.9 \times 10^{-9}$ s of HMPA molecules in the solvent cage and the intermolecular hyperfine constant value of $a = 0.08$ MHz.

It should be noted that the basic condition for EPR hyperfine structure observation in such systems is given by

$$a\tau_h > 1 \quad (22)$$

The inequality is not satisfied in the case of solvated electrons in HMPA. As a result, there is no hyperfine structure in the EPR spectrum of solvated electrons in HMPA at room temperature. At the same time, no paramagnetic shifts have ever been detected in the proton spectra of high-resolution NMR in this system because of line broadening. Thus, DNP measurements represent a valuable experimental approach to the measurement of weak hyperfine couplings under these conditions.

5. Summary and Conclusion

The pulsed DNP method gives us a way to obtain quantitative information about the individual contact as well as intermolecular dipole–dipole cross-relaxation processes that occur during molecular collisions in liquids. It provides valuable molecular–kinetic information without the need to perform any variable frequency or temperature measurements. The suggested scheme for determining CR transition probabilities can be applied to any nuclear–electronic molecular modulation mechanism. Pulsed DNP can be used as a sensitive approach for the study of very weak hyperfine interactions that cannot be detected by traditional magnetic resonance methods, such as direct observation of hyperfine structure in EPR or paramagnetic shift measurements in NMR.

Acknowledgment. The research was supported in part by a grant from the NIH (GM42208 to R.B.C.) and used facilities of the Illinois EPR Research Center (NIH P41-RR01811).

References and Notes

- (1) Bloembergen, N.; Shapiro S.; Pershau, P. S.; Artmann, J. O. *Phys. Rev.* **1959**, *114*, 445.
- (2) Tsentolovich, Y. P.; Yurkovskaya, A. V.; Frantsev, A. A.; Doctorov, A. B.; Sagdeev, R. Z. *Z. Phys. Chem.* **1993**, *182*, 119.
- (3) Batchelor, S. N.; Fischer, H. *J. Phys. Chem.* **1996**, *100*, 556.
- (4) Abragam, A. *Nuclear Magnetism*; Oxford University Press: Oxford, 1961; Chapter 8.
- (5) Hausser, K. H.; Stehlik, D. *Adv. Magn. Reson.* **1969**, *3*, 79.
- (6) Slichter, C. P. *Principles of Magnetic Resonance*; Harper and Row: New York, 1963.
- (7) Odintsov, B. M. *EPR News Lett.* **1995**, *7*, 29.
- (8) Odintsov, B. M.; Fedotov, V. N. *Preprint N 2918-77 Zavoisky Phys.-Techn. Inst.*; Russia Academy of Sciences, 1977.
- (9) Kooser, R. G.; Volland, W. V.; Freed, J. H. *J. Chem. Phys.* **1969**, *50*, 5243.
- (10) Ferrar, T. C.; Becker, E. D. *Pulse and Fourier Transform NMR*; Academic Press: New York, 1971; p 43.
- (11) Edwards, P. P. *J. Phys. Chem.* **1984**, *88*, 3772.